



INVESTIGATION OF UNAUTHORIZED CONNECTION TO ELECTRICAL NETWORKS, FAILURE TO DETECT THEIR PHASE INTERRUPTIONS AND SHORT CIRCUITS TO GROUND

N. Narzullo Mirzoyev

Ph D., Senior lecturer of the Bukhara
Institute of Engineering and Technology "Energoaudit Department",

O. Hasan Sayfiyev,

Assistant of the Bukhara Institute of Engineering and
Technology "Energoaudit Department",

T. Otabek Temirov,

Masters of Bukhara Institute of Engineering and
Technology "Energoaudit Department".

ANNOTATION

Descriptions of the principle scheme and elements of the device for detecting unauthorized connection to electrical networks, their phase breaks and short circuits to the ground are given.

Basic phrases: phase, current transformer, model, sumilink, wave, current, voltage, frequency, electrical network.

At the stage of modeling the interruptions in phase A, the operation of the electric distribution network in the maximum mode and the determinal values of consumer loads are calculated. In this research work, the calculations were made according to the calculation program.

In the modeling of phase interruptions, the values of the active resistance of the earth are taken in the range of 1 - 5 Ohm. The lower limit of the acceptable resistance range is chosen to be off from the standard supply value for high-voltage electrical networks, which is 0.5 Ohm. The upper limit of the measurement range is disabled based on the resistance values of high-power consumers [1].

Measurement values and calculation results are presented below in Table 1.1 and Figures 1.1, 1.2, 1.3. These numbers show the dependence of the cataclysms calculated from the phase break in the intervals: 1 – 2 in red, 6 – 7 in blue, 12 – 13

in black and 16 – 17 in brown.

As can be seen from Figure 1.1, the overload of phase A of the transformer in the studied mode did not exceed the permissible value for it, and its value was equal to 1.4. The above shows that the phase failure cannot cause the protective device to affect the damaged line, so the unnatural mode of the line, which is dangerous from the point of view of electrical safety, can be used arbitrarily for a long time. Such regimes are particularly dangerous during high wind warning periods in areas with high overall accident rates in power plants [2].

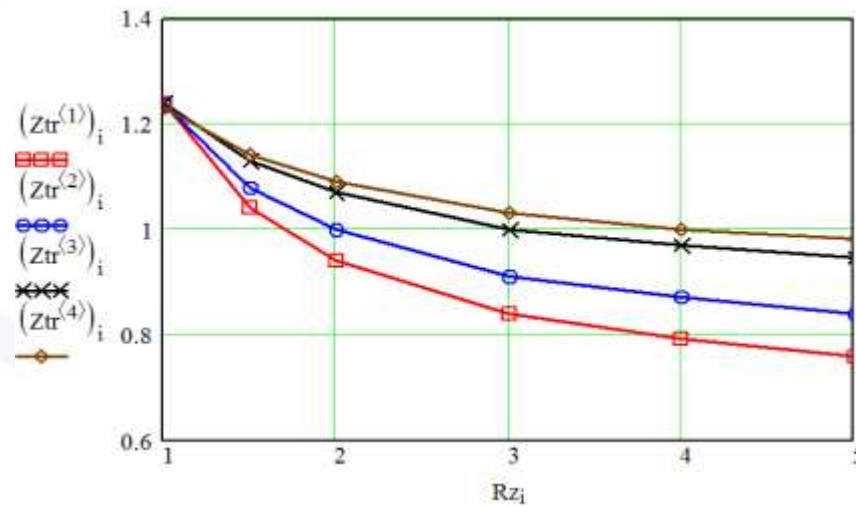


Figure 1.1 – The value of the ground resistance when the phase is broken and when it goes to ground and the dependence on the load of phase A of the step-down transformer

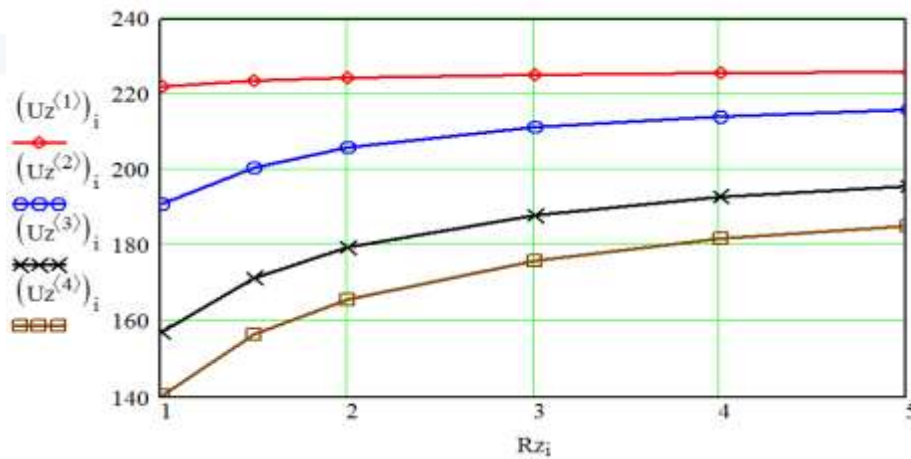


Fig. 1.2 Dependencies of the voltage at the ground connection from the value of the resistance to the ground when the phase is interrupted and falls to the ground



As can be seen from Figure 1.2, the short-circuit voltage to the ground has a maximum value and practically does not change when there is a break in the initial part of the line. When moving away from the beginning of the line, the voltage value at the point of phase interruption decreases and it depends more on the earth resistance. In all cases, the value of the voltage in the disconnected phase remains high enough and poses an obvious danger to people and animals located near the disconnected phase [3].

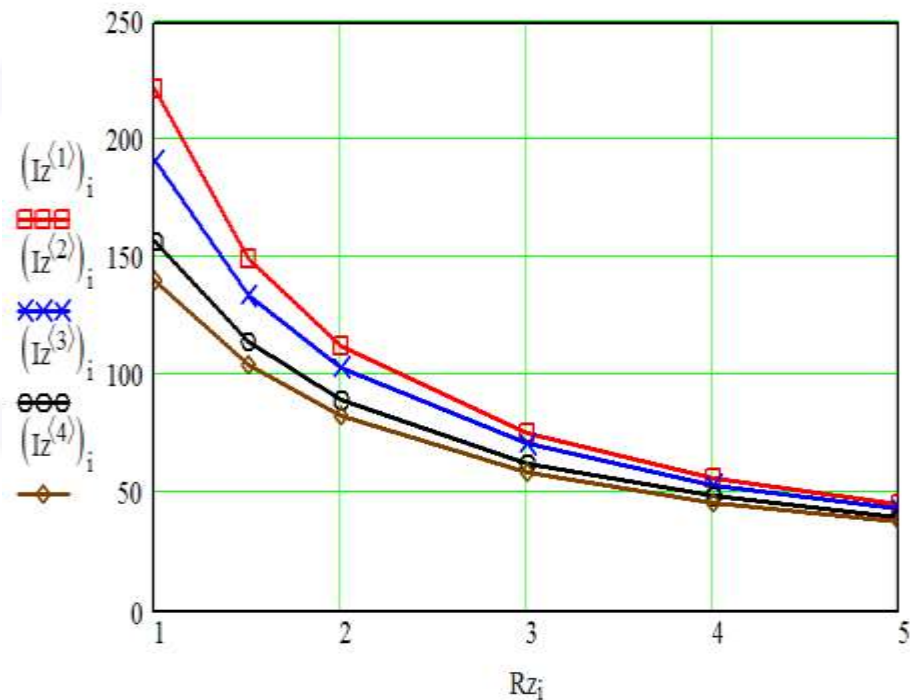


Figure 1.3 Dependence of the short-circuit current to the ground on the value of the ground resistance in the case of a phase break and its grounding

As can be seen from Figure 1.3, in the case of a phase break in different places of the line, the short-circuit current to the ground has almost the same value and depends on the value of the resistance of the ground [4]. The maximum value of the short-circuit current is when there is a break in the initial part, and the current value decreases as it moves away from the beginning of the line.

Table 1 Values of the parameters of phase failure and short circuit to the ground in different network intervals

The length of the electrical network	1 - 2	6 - 7	12 - 13	16 - 17
$R_{GND} = 1 \text{ Ohm}$				
$I_{GND}, \text{ A}$	222.1	191.0	157.1	140.3
$U_{GND}, \text{ V}$	222.1	191.0	157.1	140.3
$I_{GND}, \text{ A}$	446.7	445.6	446.6	443.8
I_{GND} / Int	1.24	1,235	1.24	1.23
$R_{GND} = 1.5 \text{ Ohm}$				
$I_{ZZ}, \text{ A}$	149.1	133.8	114.2	104.2
$U_{ZZ}, \text{ V}$	171.2	200.7	171.2	156.2
$I_{GND}, \text{ A}$	375.6	390.5	407.8	412.2
I_{GND} / Int	1.04	1.08	1.13	1.14
$R_{GND} = 2 \text{ Ohm}$				
$I_{GND}, \text{ A}$	112.2	102.9	89.6	82.8
$U_{GND}, \text{ V}$	224.4	205.9	179.3	165.6
$I_{GND}, \text{ A}$	339.8	360.9	385.8	393.6
I_{GND} / Int	0.94	1.0	1.07	1.09
$R_{GND} = 3 \text{ Ohm}$				
$I_{GND}, \text{ A}$	75.1	70.4	62.7	58.7
$U_{GND}, \text{ V}$	225.2	211.3	188.0	176.0
$I_{GND}, \text{ A}$	304.0	320.0	361.7	372.7
I_{GND} / Int	0.84	0.91	1.0	1.03
$R_{GND} = 4 \text{ Ohm}$				
$I_{GND}, \text{ A}$	56.4	53.5	48.2	45.4
$U_{GND}, \text{ V}$	225.6	214.1	192.7	181.7
$I_{GND}, \text{ A}$	286.1	314.0	348.9	361.3
I_{GND} / Int	0.79	0.87	0.97	1.0
$R_{GND} = 5 \text{ Ohm}$				
$I_{GND}, \text{ A}$	45.2	43.2	39,13	37.1
$U_{GND}, \text{ V}$	225.9	215.8	195.6	185.2
$I_{GND}, \text{ A}$	275.4	304.2	340.9	354.2
I_{GND} / Int	0.76	0.84	0.94	0.98

Calculation of phase-to-earth short-circuit currents through high resistance allowed to estimate other indicators of typical elementary sections, which allows to enter the difference between high resistance and the maximum possible phase-to-earth short-circuit currents. The current value of unauthorized connection to phases using clamps to ensure reliable power supply is determined. The most recent value of these values is 20 - 40 A.



The results obtained from the model also made it possible to determine the maximum permissible currents for developing sensitivity requirements and evaluating the error of current control devices. When summarizing the results of the model, it was found that the measurement errors do not exceed 2.5%.

Evaluation of TNQ sensitivity of the developed current control device

The value of the information signal at the TNQ output is affected by the following parameters:

the number of packages in the measuring tape;

the size of the air gap in the core;

the value of the current flowing through the conductor.

To analyze the dependence of the information signal in the form of the output voltage on the above parameters, we consider these dependencies separately: $u(d)$, $u(w)$, $u(j)$, where u is the information signal, w is the number of interconnected windings in the measuring coil w_2 , j is the current in the conductor [5].

Each parameter was estimated while keeping the others constant. The evaluation was performed at a maximum line current of 80 A for one phase of the overhead line and an air gap of 0.1 mm (0.0001 m) with two air gaps in evaluating the effect of number of windings and current. At a current of 80 A and in the evaluation of the effect of air gaps, it was carried out with the number of windings, constant ho distance and the number of windings in the evaluation of the current effect.

Based on the results of the measurement, we create sensitivity matrices of the absolute values of the main indicators of TNK.

Assessment of the effects of air pollution.

The value of the air gap, mm:

$d = [0.1 \ 0.2 \ 0.3 \ 0.4 \ 0.5 \ 0.6 \ 0.7 \ 0.8 \ 0.9 \ 1.0]$;

depending on $u(d)$:

$u_1 = [5.4574 \ 3.2568 \ 2.3210 \ 1.8029 \ 1.4739 \ 1.2464 \ 1.0798 \ 0.9525 \ 0.8520 \ 0.7077]$;

The interpolation function depends on the informational signal

the interpolation function of the dependence of the information signal on the air gap:

she is= $108.8403d^6 - 429.9242*d^5 + 687.9995*d^4 - 574.9887*d^3 + 270.0917*d^2 - 71.7501d + 10.4405$;

Derivative value:

$f1 = [-32.4562 \ -13.9632 \ -6.5181 \ -3.9600 \ -2.9356 \ -2.1167 \ -1.4154 \ -1.2015 \ -1.5178 \ -1.2974];$

Interpolation error $err1 = u1 - u;$

$err1 = [0.0014 \ -0.0076 \ 0.0145 \ -0.0091 \ -0.0064 \ 0.0086 \ 0.0043 \ -0.0113 \ 0.0063 \ -0.0013].$

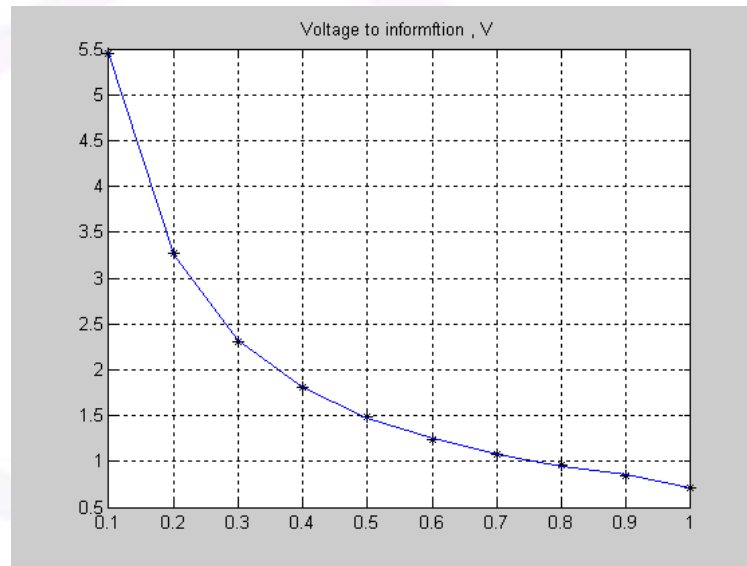


Figure 1.4 - graph of the dependence of the information signal on the size of the air gap

Evaluation of the dependence of the information signal on the number of coils in the coil

Number of chulgams:

$w = [20 \ 40 \ 60 \ 80 \ 100 \ 120 \ 140 \ 160 \ 180 \ 200];$

depends on $u(w):$

$u2 = [2.1830 \ 4.3659 \ 6.5489 \ 8.7319 \ 10.9148 \ 13.0978 \ 15.2808 \ 17.4637 \ 19.6467 \ 21.8297].$

Since the dependence of the signal on the number of windings in the coil is almost directly proportional, the proportionality coefficient k is the value of the first derivative.

$k = u2./w;$

$f2 = k = [0.1092 \ 0.1091 \ 0.1091 \ 0.1091 \ 0.1091 \ 0.1091 \ 0.1091 \ 0.1091 \ 0.1091 \ 0.1091].$

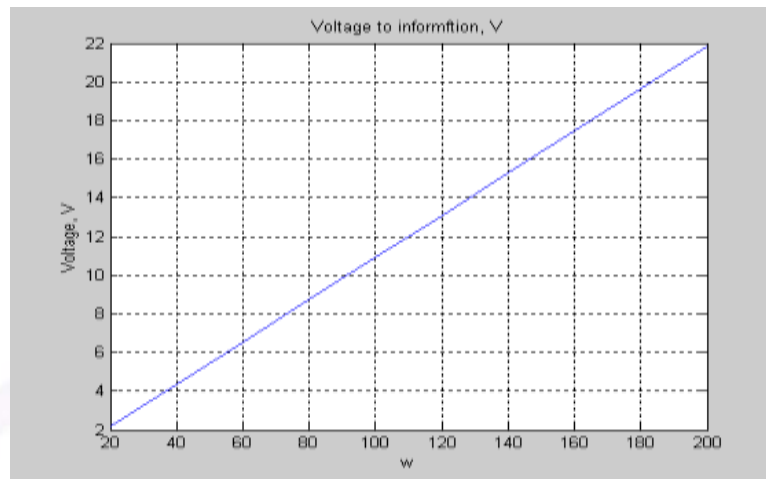


Figure 1.5 - graph of information signal dependence on the number of coils in the coil

Otsenka zavisimosti informationnogo signala ot toka v silovom prrove.

Evaluation of the dependence of the information signal on the current flowing from the conductor

t flowing through the conductorok value:

$j = [1 \ 5 \ 10 \ 20 \ 30 \ 40 \ 50 \ 60 \ 70 \ 80]$;

output information signal:

$u_3 = [2.1830 \ 4.3659 \ 6.5489 \ 8.7319 \ 10.9148 \ 13.0978 \ 15.2808 \ 17.4637 \ 19.6467 \ 21.8297]$;

primary difference:

$D = [2.1829 \ 2.1830 \ 2.1830 \ 2.1829 \ 2.1830 \ 2.1830 \ 2.1829 \ 2.1830 \ 2.1830]$

$f_3 = 2,1830$.

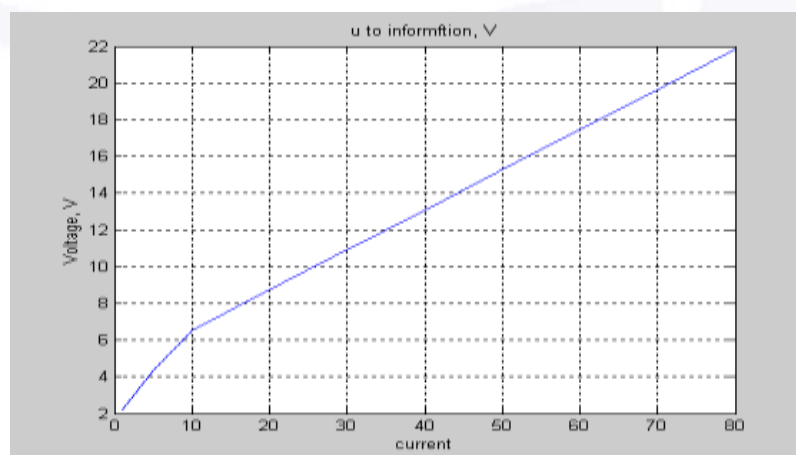


Figure 1.6. The graph of the dependence of the output information signal on the magnitude of the current flowing from the transformer



Using the information obtained above and the general differential concept, the total value of the information signal at the output is equal to the following.

$$du = \frac{du}{dd} \Delta d + \frac{du}{dw} \Delta w + \frac{du}{dj} \Delta j,$$

$$\text{Here } \frac{du}{dw} = 0.1091; \frac{du}{dd} = 32.4562; \frac{du}{dj} = 2.1830.$$

Posle podstanovki dannix (maximally absolute production value and significant error parameters) we can open the absolute elimination of the informational signal

After data exchange, we determine the absolute deviation of the signal based on errors as follows.

$$du = 32.4562 * 0.0001 + 0.1091 * 0.1 + 2.1830 * 0.1 = 0.2325.$$

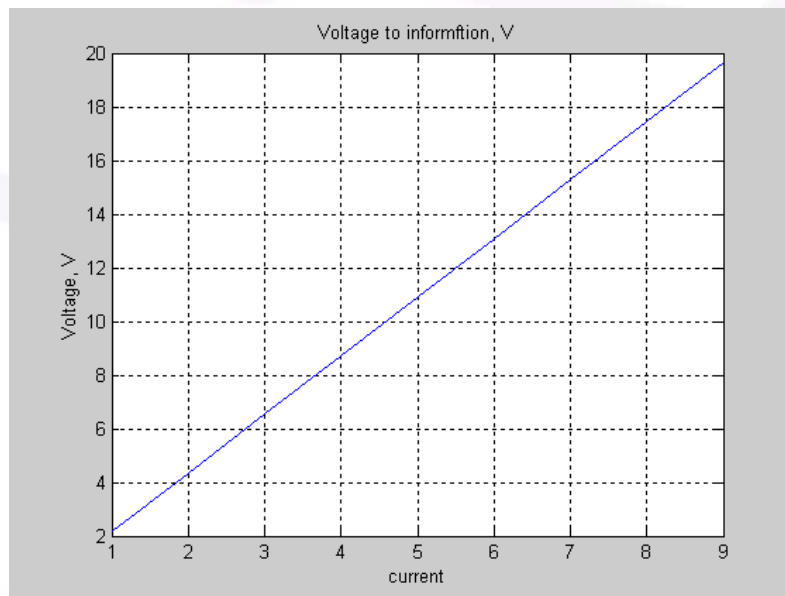


Figure 1.7 is a deviation graph of the linearity of the output signal as a function of the current.

Absolute error If we take into account external influences on TNQ, the error of the output signal will be $du = 32.4562 * 0.0001 + 0.1091 * 0.1 = 0.0142$ V.

With the help of the sensitivity matrices of the device, it is possible to obtain detailed information about the changes in the output signal for such calculations.

Modeling parts of a single phase of a distribution network in the Electronics Workbench package

The technical capabilities provided by the Electronics Workbench package allow you to develop a model of parts of a real distribution network and to study in this model different operating modes of the network, in particular, normal operation in the presence of an unauthorized connection to the electrical network [6]. In the network, when there is a single-phase earth short circuit, when there is a phase break, this model was built to check its isolation control capability, to identify the emergency modes at the beginning of the network.

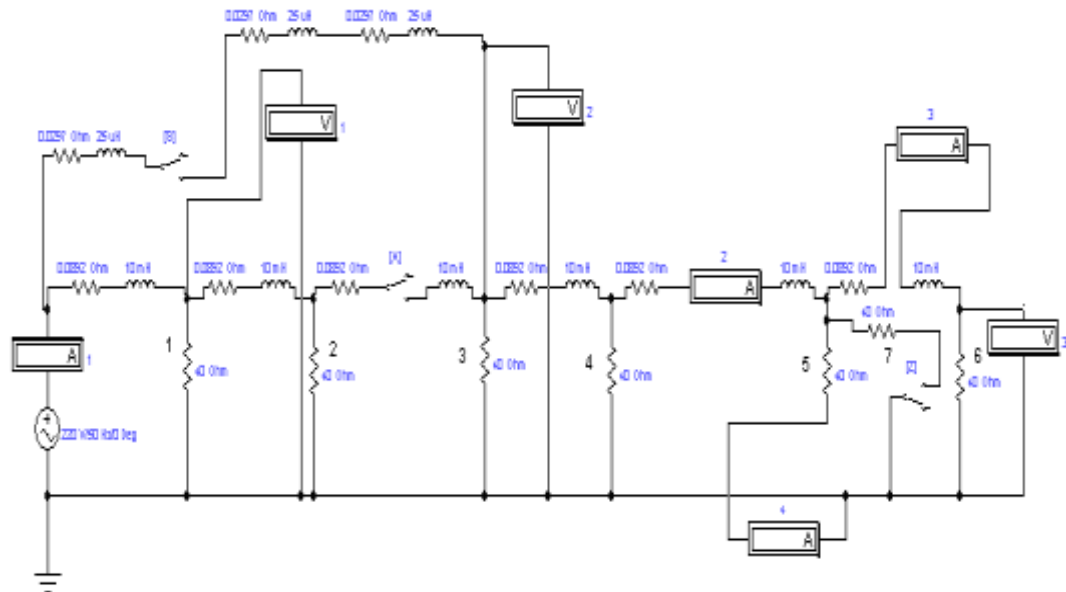


Figure 1.8. A study model of single-phase parts of a distribution network in the Electronics Workbench package

Figure 1.8 shows the model of one phase of the studied network. In the model scheme, elements whose parameters are equal to the real parameters occurring in the network are used.

Simulation of different modes is done with different combinations using S and Z keys. The simulation of additional resistances (overload, short circuit to earth and insulation control) is done by turning the Z button on and off. The position of the Z button is controlled by pressing the Z button. The shunt is connected and disconnected using the S button. .

Sample test results for different modes in the considered network are presented in Table 3.4.



The following conditions were checked:

1. The keys S and Z are open, i.e. shunt and unauthorized load off.
2. The S button is on, the Z button is off, that is, the shunt is on, the switched load is off.
3. The S button is off, the Z button is on, that is, the false load is on and the shunt is off.
4. The switches S and Z are included, which means that both the shunt and the amperage are on.
5. The state of the phase is simulated by pressing the A button (the A button is off - phase failure, the A button is on - the network works in normal mode).

Analysis of the simulation results shows that the phase break is characterized by the absence of readings from ammeters A2, A3 and A4. With switch A turned on (describing the shunt state), the voltage increase at the third consumer is 1.3 V and at the end of the line (V3) is 0.4 V [7].

Table 1.2 Results of testing the power grid modes in the model

In the presence of an unauthorized connection (the Z switch is on), the readings of the ammeters connected to node 5 indicate that Kirchhoff's first law is not fulfilled. In fact, in this case, the expression of Kirchhoff's first law should be similar to the ratio between the device indicators.

$$A2 = A3 + A4,$$
$$10.83 = 5.414 + 5.418.$$

The discrepancy in instrument readings is 0.002 A.

In the presence of theft, inconsistency.

$$A2 - (A3 + A4) = 16.19 - (5.394 + 5.398) = 5.398 \text{ A.}$$

This value is the theft value, which is much larger than the discrepancy in the readings of the ammeters when the switch Z is turned off.

The theft value of 0.1 A is more accurately determined, which is 2% of the nominal consumer load of 5 A. The same results were obtained during full-scale tests of the main converter model of the current controller under development. In this case, the ratio of the network current increase to the voltage increase at the output of the primary converter was taken into account.

In a real network, the length of the distance between the consumer connections of one phase is equal to three times the length of one span. In the simulated case, a span length of AC-35 wire of 35 mm² and 35 m was obtained. In the model, the



length of the distance between the connections of single-phase consumers is three times the length of the interval considered above. The obtained results are presented in Table 1.3.

Table 1.3
Results of testing the power grid modes in the model

Keys	Status of keys	Network operating modes	Indicators of measuring instruments						
			A1	A2	A3	A4	V1	V2	V3
A	+	There is no phase break	19.9	6,264	3,326	3,143	180.3	136.6	125.0
	-	Phase break	10.71	0.0	0.0	0.0	215.0	0.0	0.0
S	+	A shunt is connected	31.01	9.98	4,982	5,008	218.0	217.6	199.3
	-	The shunt is off	19.9	6,264	3,126	3,143	180.3	136.6	125.0
Z	+	There is theft	19.84	7,919	2,632	2,646	176.4	122.0	105.3
	-	No theft	19.9	6,264	3,126	3,143	180.3	136.6	125.0

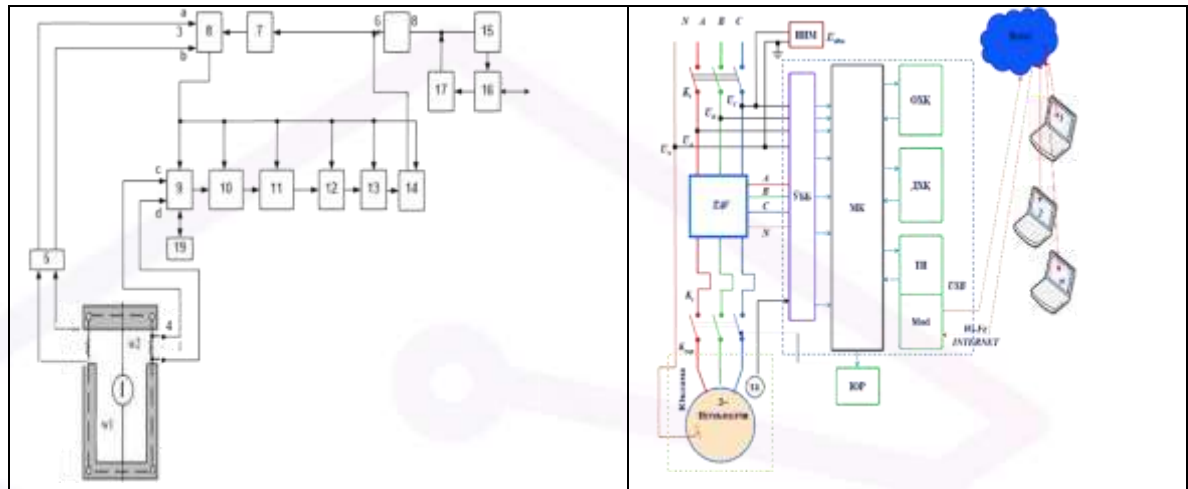
The proposed current control device is based on the task of creating improved AC converters designed to operate on the basis of digital signals, for remote transmission of the current value over the Internet in the controlled sections of the transmission line. . In this case, it is necessary to use modern components that allow non-contact measurement of currents and transmission of measurement results via a wireless network. The developed device is a converter that converts the current into a voltage signal at the output. Consists of data transmission and reception devices, microcontroller, analog-digital converters, amplifier and non-contact triggers [8, 9, 10].

The control unit includes transmitting, receiving-transmitting devices, an amplifier whose output is connected to a transmitter, whose output is connected to a transmitting-receiving modem, and a microcontroller. The other output of the microcontroller is connected to the input of the local power network.

The simplified block diagram of the current control device shown in Figure 1.9 shows the following designations:

- 1 – magnetic core of current transformer; 2 - magnetic switch of the converter; 3-5 DC network; 4 - w2 secondary converter; 5 - rectifier; 6, 18 – data reception and transmission device; 7 - Load receiving device; 8 – current control device; 9 -

rectifier; 10 – signal selection, analysis and signal matching blocks; 11 - ARO'; 12 - microcontroller; 13 - modem; 14 – high power amplifier; 15 – device receiving load from the current control device; 16 – data transfer IMS; 17 - high power amplifier, 19 - selective amplifier.



1.9 - picture. A simplified block diagram of a current control device
The circuit diagram of the network data receiver is shown in Figure 1.10.

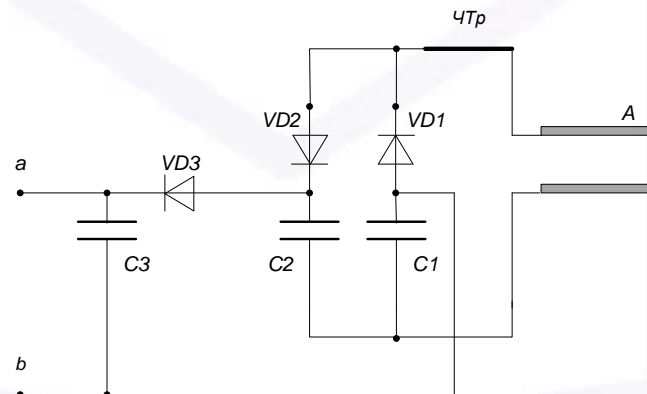


Figure 1.10. Electrical diagram of the network data receiver

In Figure 1.10, the following symbols are accepted: A - antenna; ChTR - half-cycle transformer; VD1÷VD3 – diodes; C1÷C3 - capacitors.

A current transformer J, consisting of a magnetic conductor 2 and a core 1, measures the current. The converter is made up of two coils, with w1 the primary coil running 5 and w2 the second using 9. Rectifiers provide constant current to the entire device circuit with a voltage of 2.5 to 5 V.

The current control device includes 6-data transceiver, 7-control signal receiver, 5-power source, 2-primary transformer, 8-switch, 9-rectifier, 11- ARO', 12 13-microcontroller, 14-UCh power amplifiers included.



The control part of the current control device includes a 6-transmitting device, 16-microcontroller, 17-high-frequency power amplifier and 15-transmitting device.

The case of the device is made removable. It is convenient to install electrical wires in the device. The device is hermetically protected from moisture and precipitation, it works in the temperature range from -60 to +125 °C.

Any microcontrollers, AROs, data transmission and reception devices with suitable characteristics can be used in the device.

References

1. Mirzoyev NN Information software and devices for energy efficiency management and control // Chemical Technology. Control and Management. Tashkent, Vol. 2021. No. 5, pp. 68-75. DOI:[https://doi.org/10.51346/tstu-02.21.5-77-0044.\(05.00.00;No. 12\)](https://doi.org/10.51346/tstu-02.21.5-77-0044.(05.00.00;No. 12)).
2. Mirzoyev NN Analogical Model Development Methodology For Mathematical Modeling Of Energy Efficiency Control System // The American Journal of Engineering and Technology. USA Texas,2020. Vol. 02, pp. 55-61. doi:[https://doi.org/10.37547/tajet/Volume02Issue10-10.\(Journal Impact Factor, SJIF 2022: 6,456\)](https://doi.org/10.37547/tajet/Volume02Issue10-10.(Journal Impact Factor, SJIF 2022: 6,456)).
3. Mirzoyev NN Intelligence devices for monitoring and control of energy efficiency of enterprises // Chemical Technology. Control and Management. Tashkent, Vol. 2020. Special issue 5-6, pp. 172-181. DOI:[https://doi.org/10.34920/2020.5-6.172-180.\(05.00.00;No. 12\)](https://doi.org/10.34920/2020.5-6.172-180.(05.00.00;No. 12)).
4. Siddikov Ilkhomjon, Abubakirov Azizjan, Yuldashev Azimjon, Babakhova Gulziba, IM Khonturaev, NN Mirzoev. Methodology of calculation of techno-economic indices of application of sources of reactive power// European scientific review, 2018, pp. 248-251.
5. MI Makhmudov, ZE Kuziev, SS Nurov, SS Sidikov "Optimal ratio of primary and secondary clarifier characteristics in wastewater treatment plants". Chemical technology control and management, 2020, No. 4 (94), pp. 5-10.
6. MI Makhmudov, ZE Kuziev, SS Nurov, SS Sidikov "Analysis and comparison of optical and mass methods of measuring active sludge concentration in wastewater treatment". Journal of critical reviews, vol 7, issue 11, 2020, pp. 3050-3057.



7. MI Makhmudov, ZE Kuziev, SS Nurov, SS Sidikov " Assessment of energy saving capabilities in air blowers of biological wastewater treatment plants ". Journal of critical reviews, 2020, No. 7 (11), pp. 3058-3066.
8. MI Makhmudov, ZE Kuziev, SS Nurov, SS Sidikov "Analysis of the Process of Aerobic Stabilization of Sediment on the Example of Purification Facilities of the Republic of Uzbekistan". Annals of RSCB, ISSN:1583-6258, 2021, Vol. 25, Issue 3, pp. 7094 – 7105.
9. MI Makhmudov, ZE Kuziev, SS Nurov, SS Sidikov "Review and analysis of methods for measuring concentration of suspended substances and active sludge during biological treatment of waste water".Scientific-technical journal: 2021, Vol. 4: Iss. 3, pp. 27-33.
10. MI Makhmudov, ZE Kuziev, SS Nurov, SS Sidikov "Assessment of energy saving capabilities in air blowers of biological wastewater treatment plants". European journal of molecular & clinical medicine, 2020, #7 (06), pp. 1474-1486.